

# Climate and carbon cycle changes under the overshoot scenario

Jesse Nusbaumer<sup>a</sup>, Katsumi Matsumoto<sup>b,\*</sup>

<sup>a</sup> *Earth and Atmospheric Science, Purdue University, 550 Stadium Mall Dr. West Lafayette, IN 4790, USA*

<sup>b</sup> *Geology and Geophysics, University of Minnesota, 310 Pillsbury Dr. SE, Minneapolis, Minnesota, 55455 USA*

Received 30 August 2007; accepted 14 January 2008

Available online 30 January 2008

## Abstract

The “overshoot scenario” is an emissions scenario in which CO<sub>2</sub> concentration in the atmosphere temporarily exceeds some pre-defined, “dangerous” threshold (before being reduced to non-dangerous levels). Support for this idea comes from its potential to achieve a balance between the burdens of current and future generations in dealing with global warming. Before it can be considered a viable policy, the overshoot scenario needs to be examined in terms of its impacts on the global climate and the environment. In particular, it must be determined if climate change caused by the overshoot scenario is reversible or not, since crossing that “dangerous” CO<sub>2</sub> threshold could result in climate change from which we might not be able to recover. In this study, we quantify the change in several climatic and environmental variables under the overshoot scenario using a global climate model of intermediate complexity. Compared to earlier studies on the overshoot scenario, we have an explicit carbon cycle model that allows us to represent carbon-climate feedbacks and force the climate model more realistically with CO<sub>2</sub> emissions rates rather than with prescribed atmospheric *p*CO<sub>2</sub>. Our standard CO<sub>2</sub> emissions rate is calculated on the basis of historical atmospheric *p*CO<sub>2</sub> data and the WRE S650 non-overshoot stabilization profile. It starts from the preindustrial year 1760, peaks in the year 2056, and ends in the year 2300. A variety of overshoot scenarios were constructed by increasing the amplitude of the control emissions peak but decreasing the peak duration so that the cumulative emissions remain essentially constant. Sensitivity simulations of various overshoot scenarios in our model show that many aspects of the global climate are largely reversible by year 2300. The significance of the reversibility, which takes roughly 200 years in our experiments, depends on the time horizon with which it is viewed or the number of future generations for whom equity is sought. At times when the overshoot scenario has emissions rates higher than the control scenario, the transient changes in atmospheric and oceanic temperatures and surface ocean pH can be significant, even for moderate overshoot scenarios that remain within IPCC SRES emissions scenarios. The large transient changes and the centennial timescale of climate reversibility suggest that the overshoot might not be the best mitigation approach, even if it technically follows the optimal economic path.

© 2008 Elsevier B.V. All rights reserved.

**Keywords:** overshoot scenario; climate change; carbon cycle; numerical model

## 1. Introduction

Climate change is arguably the most significant international environmental policy challenge facing us today. A goal of the United Nations Framework Convention on Climate Change (UNFCCC) is to stabilize greenhouse gas concentrations in the atmosphere at a level that would prevent “dangerous anthropo-

genic interference” with the climate system. Policy makers have to attempt to accomplish this goal while minimizing damage or disruption to other areas of concern, such as the economy. One of the difficulties in achieving this goal is the lack of consensus on what “dangerous” anthropogenic interference is, which can vary among different groups that have different values (Schneider and Mastrandrea, 2005).

An important issue that must be considered in this debate is intergenerational equity, because global warming is not an inter-annual or even decadal phenomenon, but is instead more of a centennial phenomenon. For example, even if anthropogenic CO<sub>2</sub> emissions are halted now, warming will continue until planetary

\* Corresponding author. Tel.: +1 612 624 0275; fax: +1 612 625 3819.

E-mail address: [katsumi@umn.edu](mailto:katsumi@umn.edu) (K. Matsumoto).

radiative equilibrium is established. This will take centuries, given the large heat capacity of water and therefore the slow thermal response of the oceans (Hansen et al., 2005). The long time horizon means that our action today or lack thereof will impact future generations, who have yet to arrive and whose interests are difficult to represent.

In a recent article, Huntingford and Lowe (2007) discussed the concept of the “overshoot scenario” as a possible means to achieve some sense of equity in the burdens of the current generations versus burdens of future generations when dealing with global climate change. According to this concept, the current generations will bear the large burden of having to significantly reduce fossil fuel consumption if they decide to stabilize future atmospheric CO<sub>2</sub> and thus global climate. On the other hand, if little or no action is taken to curb CO<sub>2</sub> emissions now, then future generations will bear the burden of dealing with the consequences of a warmer climate. In the overshoot scenario, emissions would be reduced moderately in the short term but more sharply later on, when compared to a non-overshooting scenario. This is akin to a recent description of the optimal economic path to take as predicted by a mainstream economic model (Nordhaus, 2007). As characterized by Huntingford and Lowe (2007), the overshoot scenario could be “a conscious policy that removes some of the burden of mitigation from the present generations while protecting future generations from exposure to the most severe impacts.”

A major uncertainty associated with the overshoot scenario is climate reversibility. That is, would exceeding a certain atmospheric CO<sub>2</sub> concentration cause the climate to enter a state from which recovery becomes impossible? Another concern is the severity of transient climate change during the time of overshoot, even if the transient behavior itself is reversible in the long term.

To our knowledge, there have been two publications based on the same set of numerical modeling experiments that have examined the overshoot scenario concept (Nakashiki et al., 2006; Tsutsui et al., 2007). The experiments employed the Community Climate System Model 3, the latest of the NCAR atmosphere–ocean coupled climate models (Collins et al., 2006). Their overshoot forcing function consists of a combination of two IPCC SRES atmospheric *p*CO<sub>2</sub> stabilization scenarios (Nakicenovic et al., 2000), where the overshoot is defined by an increasing *p*CO<sub>2</sub> in the higher *p*CO<sub>2</sub> scenario followed by a sudden and discontinuous drop to a lower *p*CO<sub>2</sub> scenario. The foci of their studies include the transient response of the Atlantic meridional overturning circulation (MOC) (Nakashiki et al., 2006) and surface air and ocean temperatures (Tsutsui et al., 2007). These studies find that both MOC and surface temperatures are largely reversible within 100 years of the overshoot.

In this study, we build on these studies and further explore the consequences of the overshoot scenario within a framework of a global climate-carbon model of intermediate complexity. Our study is distinct in that we have an explicit carbon model coupled to our climate model. This allows us to force the climate model more realistically with CO<sub>2</sub> emissions rather than with prescribed atmospheric *p*CO<sub>2</sub>, thereby realizing the climate-carbon feedback. In addition to MOC and temperature, we examine ocean acidification as well as changes in the CO<sub>2</sub> exchange between the oceans and atmosphere.

## 2. Model description

The global climate-carbon model that we use in this study is GENIE-1. The physical climate model consists of a 3-dimensional dynamical model of the ocean, a 2-dimensional dynamic-thermodynamic model of sea ice, and an energy and moisture balance model of the atmosphere (Edwards and Marsh, 2005). The model is efficient, which is in part due to its coarse resolution with 8 vertical levels and 32 × 32 horizontal grid. The model has been objectively calibrated by ensemble model runs so that the cost function, defined with observed atmospheric surface temperature, humidity, oceanic temperature, and salinity, is minimized. We use the set of physical model parameters thus optimized and described by Edwards and Marsh.

The behavior of the meridional overturning circulation (MOC), a key feature of ocean general circulation models, is fairly well documented in GENIE (Marsh et al., 2004; Lenton et al., 2007; Marsh et al., 2007). As in other models, MOC in GENIE exhibits the usual hysteresis behavior in response to freshwater forcing. Due to the fast run time of GENIE, Marsh and colleagues have been able to investigate its MOC response systematically in ensemble runs that can sweep large parameter spaces (Marsh et al., 2004; Marsh et al., 2007).

The carbon or biogeochemistry model has complete seawater carbon chemistry (Ridgwell et al., 2007). Its biological production at the surface is driven by Michaelis–Menton nutrient kinetics based on nutrient phosphate and limited by light and sea ice cover. In addition to phosphate, prognostic variables in the carbon model include dissolved inorganic carbon (DIC), alkalinity, and oxygen. Air–sea exchange of CO<sub>2</sub> is driven by a partial pressure gradient (*p*CO<sub>2</sub>) across the air sea interface and is dependent on the wind speed squared (Wanninkhof, 1992). As with the physical model, the carbon model has been calibrated by minimizing the cost function defined with alkalinity and phosphate (Ridgwell et al., 2007). Our model simulations that include CO<sub>2</sub> radiative feedback show that the model’s mean surface air temperature increases by approximately 2.6 °C per doubling of CO<sub>2</sub>. This is in the lower part of the published range of 1.5–4.5 °C per doubling of *p*CO<sub>2</sub> as summarized by the IPCC (Forster et al., 2007). The focus of this study is the atmosphere–ocean climate system, and so our carbon model does not represent any land-based vegetation. Processes and feedbacks associated with it are therefore not accounted for here.

## 3. Experiment design

The non-overshoot control run in this study is based on a 541-year CO<sub>2</sub> emissions rate, which is calculated from our model simulation with atmospheric CO<sub>2</sub> prescribed to follow observations from the years 1760 to 2005 and the WRE S650 stabilization scenario from years 2005 to 2300 (Wigley et al., 1996). The S650 scenario has atmospheric CO<sub>2</sub> concentrations that continue to increase until stabilization at 650 ppm in the year 2200 (solid line, Fig. 1b). We offer two justifications for choosing S650 for our control scenario. The first is that the S650 scenario is inside the range of IPCC SRES scenarios, which are indicated by the shaded region in Fig. 1a and arguably makes our choice reasonable. The

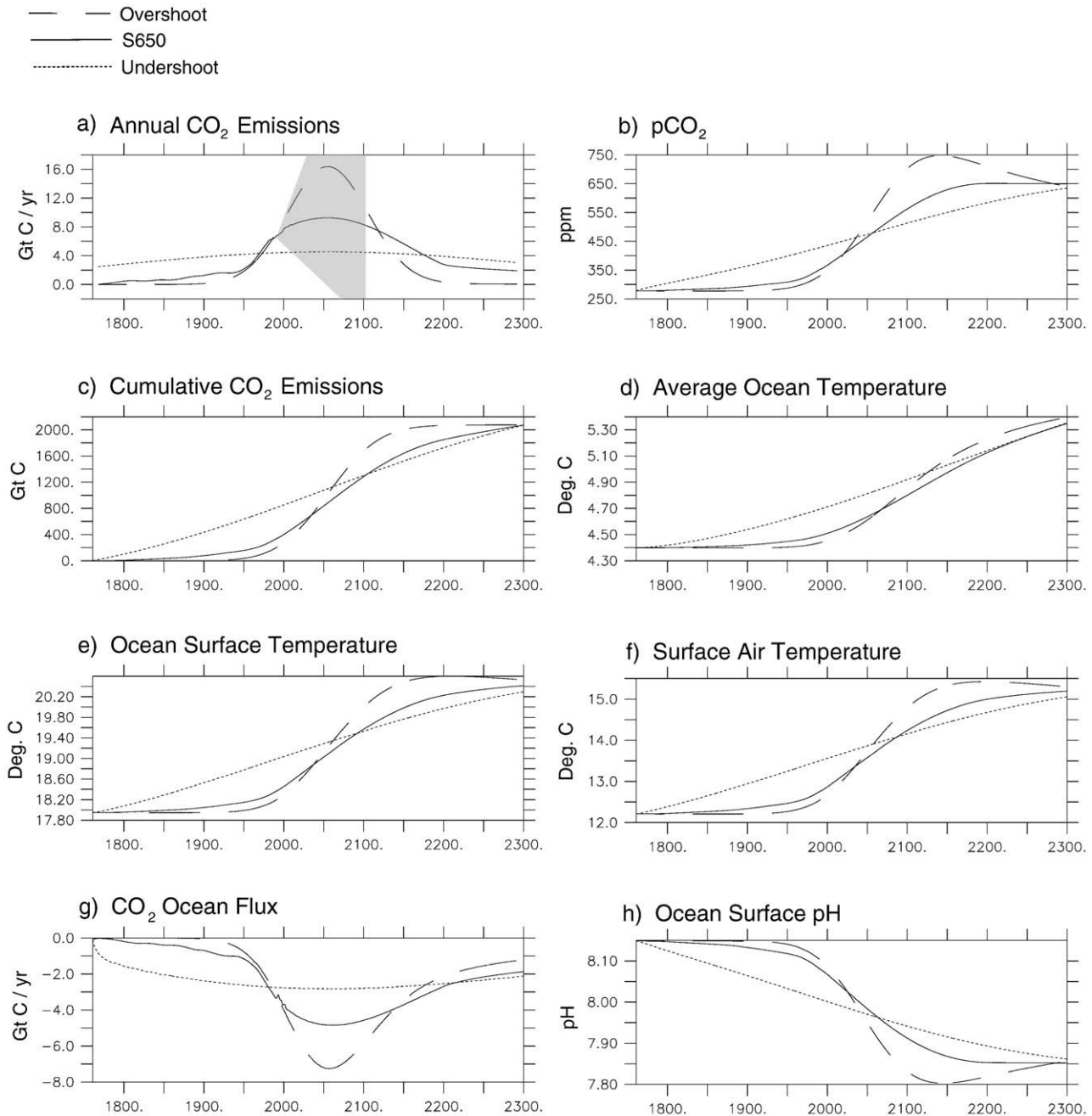


Fig. 1. Time series of the control, overshoot, and undershoot scenario simulations. Model is forced with (a) annual CO<sub>2</sub> emissions (solid line=control, dashed=overshoot, dotted=undershoot). The range of CO<sub>2</sub> emissions from the IPCC SRES scenarios is indicated by the grey shaded area and continues off the top of the plot. Model response includes: (b) atmospheric pCO<sub>2</sub>; (c) cumulative anthropogenic CO<sub>2</sub> emissions; (d) whole ocean average ocean temperature; (e) global mean sea surface temperature; (f) global mean surface air temperature; (g) air-to-ocean CO<sub>2</sub> flux; and (h) global mean ocean surface pH.

second is that, as we will demonstrate below, the qualitative results using an overshoot scenario based on the S650 scenario is similar to an overshoot scenario based on other stabilization scenarios.

In the simulation where atmospheric CO<sub>2</sub> is prescribed to follow observations and S650, the total carbon inventory in the world ocean increases as increasing atmospheric pCO<sub>2</sub> drives a net transfer of CO<sub>2</sub> from the atmosphere to the oceans. This is effectively the oceanic uptake of anthropogenic carbon. The time rate of change in the total ocean–atmosphere carbon inventory is the emissions rate required by GENIE to maintain

its atmosphere to the prescribed values while continuing to absorb carbon in the oceans (solid line, Fig. 1a). All emissions rates are given in Gt C yr<sup>-1</sup> (1 Gt=10<sup>15</sup> g).

After confirming that the two simulations forced with our control CO<sub>2</sub> emissions rate and with prescribed atmospheric CO<sub>2</sub> (observations+S650) yielded the same results, we created overshoot and undershoot scenarios using an idealized function of time that approximated the control emissions rate. It is important to realize that these overshoot scenarios are not perturbations to the prescribed scenario, but are simply set to

have the same cumulative CO<sub>2</sub> emissions as the prescribed scenario by the year 2300. The idealized function, which is a Gaussian function, is given as:

$$\text{emissions} = \left( \frac{2071 k}{\sqrt{2\pi}\sigma} \right) e^{-\frac{(x-m)^2}{2\sigma^2}} \quad (1)$$

In this equation, *emissions* is the CO<sub>2</sub> emissions rate in Gt C yr<sup>-1</sup>,  $\sigma$  is the standard deviation of the emissions time series, *m* is the mean of the emissions time series, and *k* is a constant of proportionality. The independent variable *x* is measured in years, and has a domain that goes from 1760 to 2300, which is equivalent to the time span of the prescribed control run. The best fit Gaussian function approximated the control emissions curve well enough that the cumulative CO<sub>2</sub> emissions was within 4.8 of 2071 Gt C, which is the cumulative CO<sub>2</sub> emissions of the control emissions curve, by the year 2300.

We then created overshoot as well as undershoot scenarios by changing  $\sigma$ , or by making the emissions profiles either “low variance” or “high variance”. Reducing  $\sigma$  creates an overshoot scenario (e.g., dashed line, Fig. 1a) and increasing  $\sigma$  creates an undershoot scenario (e.g., dotted line, Fig. 1a). A key constraint in creating these scenarios is that the cumulative CO<sub>2</sub> emissions must be the same for every scenario by the year 2300, 541 years after the preindustrial year 1760.

In addition to investigating climate change with GENIE, we also designed simple experiments to understand the global ocean carbon cycle, whose changes can feed back on climate. For example, the warming of sea surface temperatures will reduce CO<sub>2</sub> gas solubility, which reduces the net transfer of CO<sub>2</sub> from the atmosphere to the ocean and thereby acts as a positive feedback on global warming. Here, we have designed experiments to quantify the roles of biology and temperature on oceanic uptake of CO<sub>2</sub> by turning them “on” and “off” alternately.

#### 4. Results

Fig. 1 compares model simulations using our control emissions, an overshoot scenario, and an undershoot scenario. In the control run (solid lines), the calculated emissions rate (Fig. 1a) does indeed reproduce the prescribed atmospheric CO<sub>2</sub> that is a combination of observations and S650 (Fig. 1b). The cumulative CO<sub>2</sub> emissions by the year 2300 is 2071 Gt C (Fig. 1c). Global mean temperatures in the surface ocean (Fig. 1d), the entire world ocean (Fig. 1e), and the surface air (Fig. 1f) all increase monotonically from pre-industrial values. Surface air temperature increases from 12.2 °C to 15.2 °C by 2300; increase is slightly higher for a more extended run, giving an equilibrium climate sensitivity of 2.6 °C per CO<sub>2</sub> doubling. While surface ocean and air temperatures are beginning to stabilize by the year 2300, the average ocean temperature is still increasing relatively sharply. This is consistent with the notion that the oceans are the slowest to come to radiative equilibrium under global warming due to the high heat capacity of water (Hansen et al., 2005). The flux of CO<sub>2</sub> across the air–sea interface (Fig. 1g) is greatest when the emissions rate is greatest (Fig. 1a), thus indicating that the flux is driven primarily by the *p*CO<sub>2</sub> gradient across the interface. Finally, the surface ocean pH decreases from

8.2 in 1760 to 8.05 by 2009 and decreases to 7.9 by the year 2300. The decrease in pH of 0.1 from the preindustrial era to the present decade is consistent with the results of the Ocean Carbon Cycle Intercomparison Project Phase 2 models (Orr et al., 2005).

The overshoot emissions scenario (dashed lines, Fig. 1) was created by arbitrarily reducing  $\sigma$  in Eq. (1), while remaining within the IPCC SRES scenario family. The transient model response to this emissions forcing (Fig. 1a) in terms of atmospheric *p*CO<sub>2</sub> is a peak of 747.7 ppm in the year 2114 before eventually decreasing down to 626.7 ppm by 2300 (Fig. 1b). The transient peak is 97.1 ppm over the control run and represents an “overshoot” as envisioned by Huntingford and Lowe (2007). This peak in atmospheric CO<sub>2</sub> lags by 58 years the time of maximum CO<sub>2</sub> emissions which occurs in the year 2056. The lag indicates the response time of the upper ocean carbon cycle that depends on the CO<sub>2</sub> absorption at the surface and mixing into the interior. This lag is partly caused by the “slow”, decadal time scale of the thermocline and upper ocean ventilation, which replaces CO<sub>2</sub>-saturated surface waters with unsaturated waters from below. Another contributing factor is an increase in the atmosphere–ocean CO<sub>2</sub> disequilibrium, which seems to have been increasing since the preindustrial times until now (Matsumoto and Gruber, 2005). This 58-year lag in the ocean carbon cycle response is partly responsible for the even larger, 142-year lag of the maximum air temperature following the time of maximum CO<sub>2</sub> emissions (Fig. 1f). The temperature lag is mostly due to the slow thermal response of the ocean due to its high heat capacity (Hansen et al., 2005).

Compared to the control run, the overshoot scenario (dashed lines, Fig. 1) causes the model to respond with larger changes in magnitude, with air temperatures becoming as large as 0.6 °C warmer around the year 2128 (Fig. 1f). The larger flux of CO<sub>2</sub> into the ocean (Fig. 1g) causes more intense changes in other environmental variables, such as surface ocean pH; the maximum pH reduction (i.e., acidification) is 0.08 pH units in the year 2108 (Fig. 1h). After their respective peaks, all variables return to about the same level as the control run by the end of the run period in the year 2300.

The undershoot emissions scenario with a drastically flattened peak (dotted line, Fig. 1) was created by arbitrarily increasing  $\sigma$  in Eq. (1). It is an unrealistic example since it required us to change past emissions but is meant to provide a counterpart to the overshoot scenario as a sensitivity simulation. Atmospheric *p*CO<sub>2</sub> in the undershoot scenario reaches a maximum of 521.0 ppm in 2100 and ends with 630 ppm by 2300 (Fig. 1b). None of the other climate and environmental variables change as rapidly as the control or overshoot scenarios, with the surface air temperature being 0.3 °C lower than the control scenario by the year 2180 (Fig. 1f). The peaks in the air-to-ocean CO<sub>2</sub> flux and surface ocean pH are all quite modest comparatively (Fig. 1g, h). However, all of the climatic and environmental variables eventually reach essentially the same level as the control scenario. It is significant to realize, too, that all of differences between the control, overshoot, and undershoot scenarios are caused by the emissions pathway, and not the cumulative emissions, since they are designed to have the same total cumulative emissions by the end of the year 2300.

The spatial patterns of a few variables in the overshoot scenario run compared to the control run at the time of maximum CO<sub>2</sub>

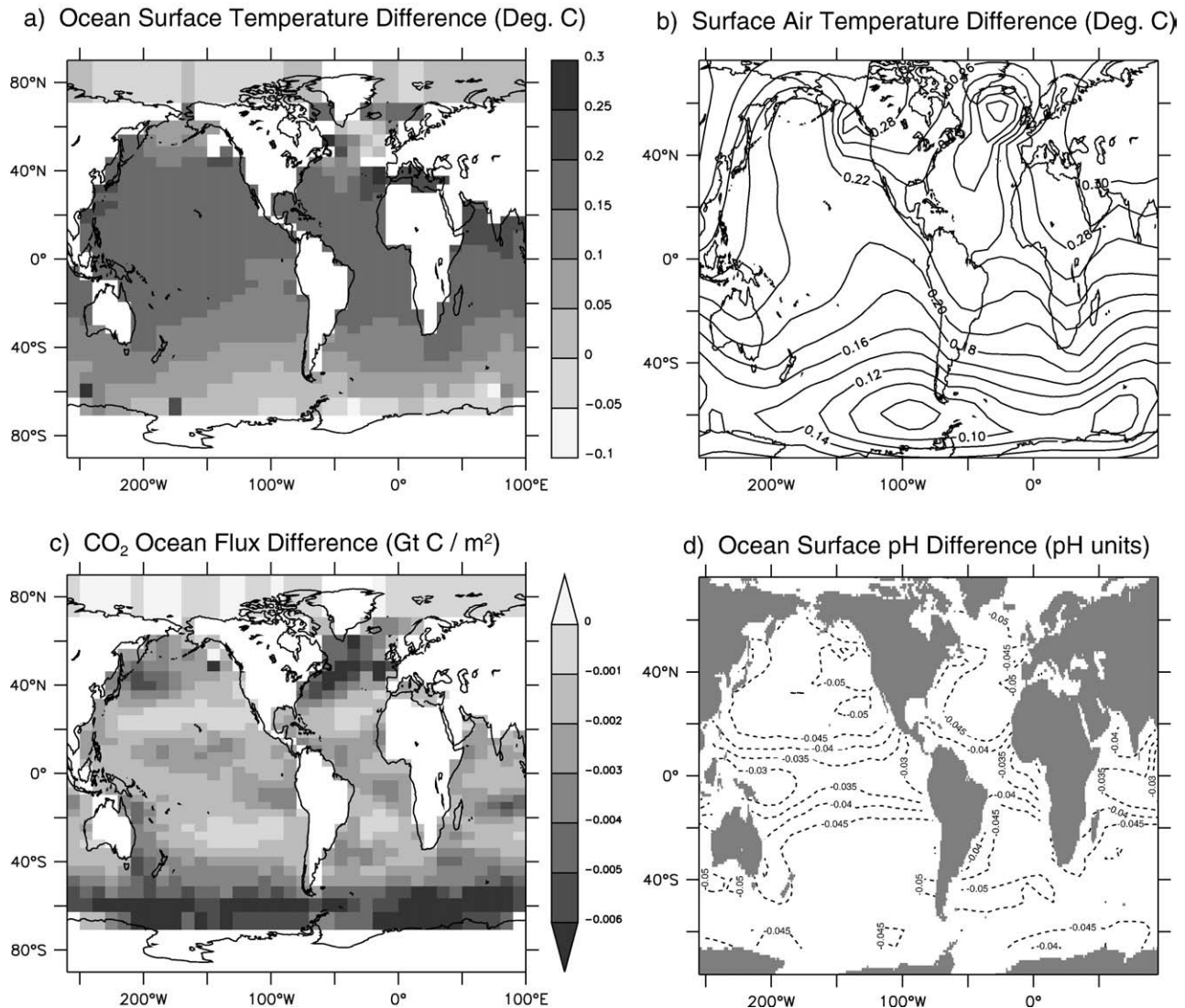


Fig. 2. Maps of overshoot minus control (i.e. WRE S650) difference at the time of maximum CO<sub>2</sub> emissions (year 2056) for (a) ocean surface temperature, (b) surface air temperature, (c) air-to-ocean CO<sub>2</sub> flux, and (d) ocean surface pH.

emissions (year 2056) is shown in Fig. 2. Ocean surface temperatures in the overshoot run is approximately 0.15 °C warmer in much of the lower and mid-latitudes (Fig. 2a). Both the Arctic Ocean and the surrounding waters of Antarctica experienced little change in temperature. The Arctic surface ocean temperature was buffered by the continual presence of sea ice in the model, although the Arctic sea ice became thinner by 0.5 m as the overlying air temperature increased by about 0.3 °C (Fig. 2b). The air temperature increases everywhere but is largest in the north; this is entirely consistent with the results of Tsutsui et al. (2007). Fig. 2c shows that the CO<sub>2</sub> flux into the ocean was greater for the overshoot scenario everywhere than for the control scenario. The increased flux is pronounced in the Southern Ocean, where the winds are strong and vertical mixing is so strong that CO<sub>2</sub>-saturated surface waters are taken down into the interior more quickly than in other areas. The increased flux of CO<sub>2</sub> causes a greater drop in surface ocean pH as it becomes more acidic (Fig. 2d). The change in pH does not correspond directly to the change in air-to-sea CO<sub>2</sub> flux, because seawater chemistry buffers

its pH from changing rapidly. The buffer capacity, technically referred to as the Revelle (buffer) factor (Takahashi et al., 1980), approximately reflects the carbonate ion (CO<sub>3</sub><sup>2-</sup>) concentration. Carbonate ion is basic and neutralizes the acidic CO<sub>2</sub> to form bicarbonate ion (HCO<sub>3</sub><sup>-</sup>). The change in pH is smaller in the low latitude surface water (Fig. 2d), because CO<sub>3</sub><sup>2-</sup> is more abundant there than in the high latitudes.

The change in MOC that accompanies global warming is all reduction, regardless of whether the CO<sub>2</sub> emissions is overshoot or undershoot (Fig. 3). The Atlantic MOC representing the North Atlantic Deep Water flow starts at 16.9 Sv (Sv = 10<sup>6</sup> m<sup>3</sup> s<sup>-1</sup>) in the control run, weakens to 12.6 Sv by 2160 before strengthening slightly to 13.2 Sv by 2300 (solid line, Fig. 3a). This transient weakening is more pronounced in the overshoot scenario (dashed line). At its weakest point, the Atlantic MOC drops to 11.5 Sv in the overshoot scenario. The change in the undershoot scenario is less dramatic but is monotonically a weakening (dotted line). The initial weakening and subsequent recovery of the Atlantic MOC under global warming in the control and overshoot scenarios are

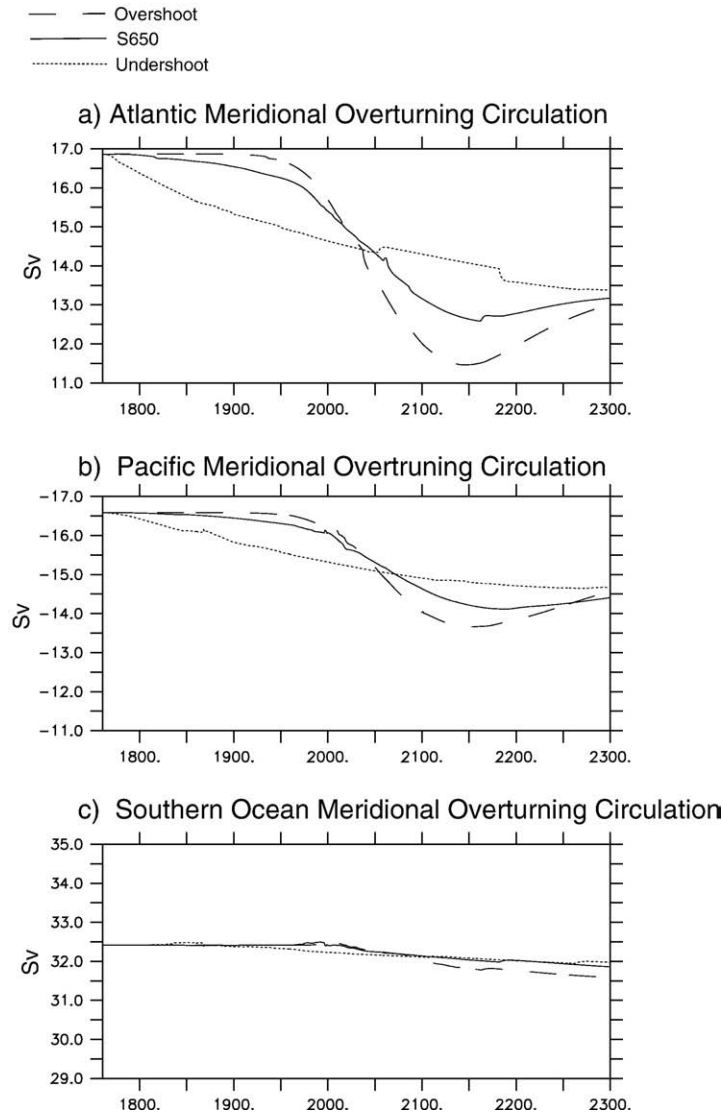


Fig. 3. Time series of the meridional overturning circulation in the control, overshoot, and undershoot scenario simulations for (a) Atlantic, (b) Pacific, and (c) Southern Ocean. The y-axis for all three panels spans 6 Sv. Solid line=control, dashed=overshoot, dotted=undershoot.

consistent with previous findings by IPCC in coupled model simulations that attributed the weakening mostly to high latitude warming (Cubasch et al., 2001) and possibly related to changes in precipitation. Marsh et al. (2007) also find that MOC is weakened in GENIE under increased atmospheric CO<sub>2</sub> forcing. Our results are also consistent with the recovery seen by Nakashiki et al. (2006) in their overshoot experiment.

The Pacific MOC largely represents a southern sourced deep water flow and has a similar response as the Atlantic MOC but is more muted overall (Fig. 3b). In both the control and overshoot scenarios, the Pacific MOC weakens temporarily before recovering slightly (solid and dashed lines, Fig. 3b). Again the response in the undershoot scenario lacks the transient weakening and is instead a slow but monotonic weakening (dotted line). The Southern Ocean MOC under the three scenarios all show slight weakening the magnitude in comparison to the Atlantic and Pacific MOC is very small (Fig. 3c).

To test whether the model response that we observed in Fig. 1 for “moderate” overshoot scenario that remained within the IPCC

SRES scenario range is robust, we conducted a model run with an “extreme” overshoot scenario (Fig. 4). By choosing an extremely low  $\sigma$  in Eq. (1), we effectively created a single “pulse” of CO<sub>2</sub> emissions (Fig. 4a). The peak emissions are almost 120 Gt C yr<sup>-1</sup> in the extreme case compared to roughly 16 Gt C yr<sup>-1</sup> in the moderate case. Despite this difference, model results from the two cases are qualitatively quite similar. For example,  $p\text{CO}_2$  peaks at 983.0 ppm in the year 2064 for the pulse scenario (dashed line, Fig. 4b), which is 487.3 ppm higher than the control scenario. However, by the year 2300, the pulse scenario’s  $p\text{CO}_2$  drops down to 652.1 ppm, only 2.1 ppm more than the control simulation. The extremely high  $p\text{CO}_2$  in the extreme scenario causes a surface air temperature warming of 1.2 °C relative to the control simulation in the year 2091 before dropping to 0.2 °C by 2300. Although we do not show this, the Atlantic MOC in the “extreme” case is very similar to the “moderate” case shown in Fig. 3. In the extreme case, the Atlantic MOC reaches a minimum of 10.1 Sv in the year 2105 before recovering to 12.8 Sv by the year 2300, which is close to the “moderate” case of 13.2 Sv, although still

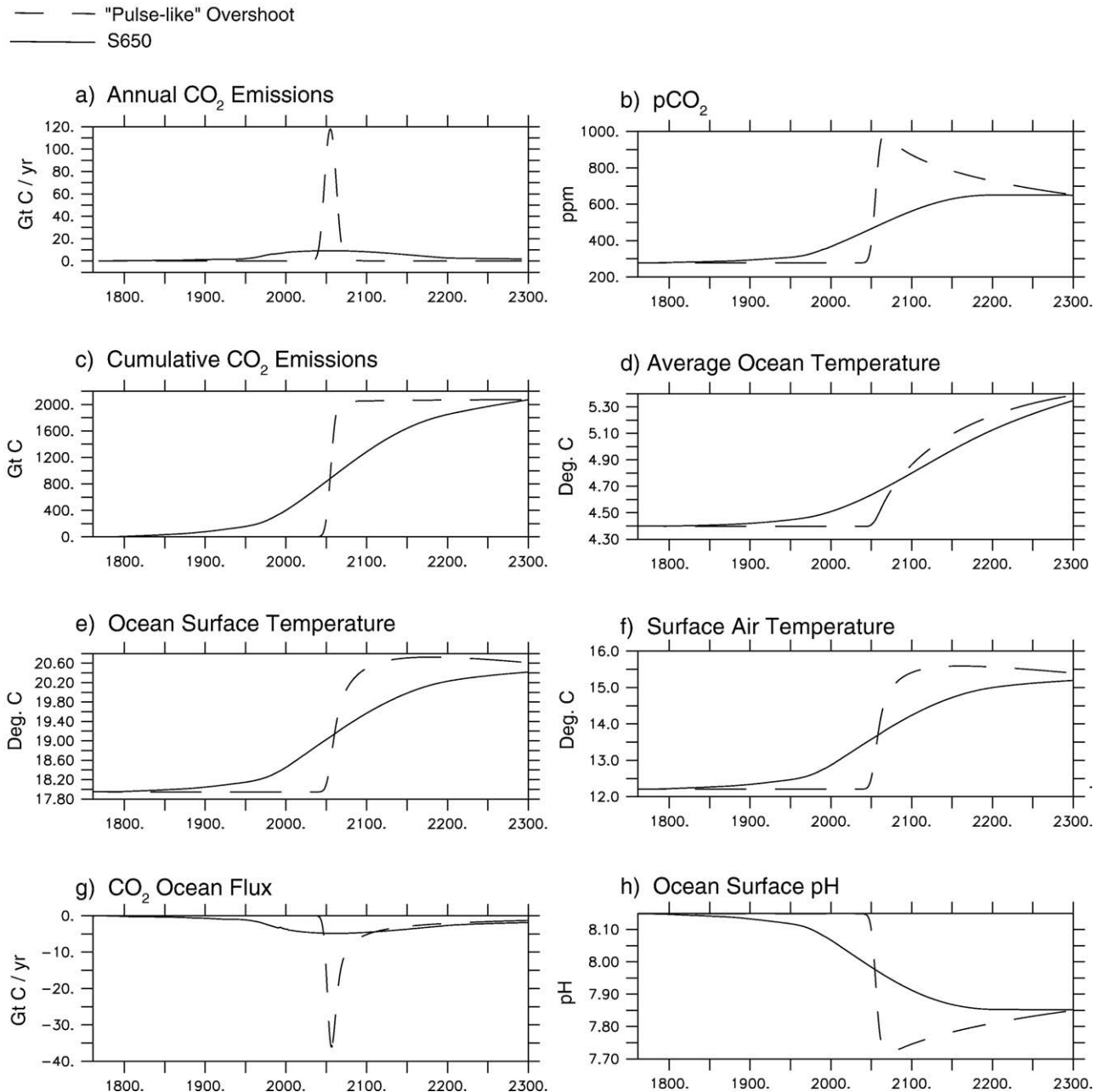


Fig. 4. Time series of "extreme" overshoot and control simulations as in Fig. 1. Solid line=control, dashed=extreme overshoot.

somewhat lower. The Pacific and Southern Ocean MOC changes look almost identical for both the "extreme" and "moderate" overshoot scenarios. This again shows that overshoot scenarios do eventually return to the control scenario levels, but not before going through many decades of elevated warming. This experiment also supports our assumption that overshoot scenarios based on stabilizing concentration scenarios will likely give the same qualitative model response.

In the last set of experiments, we investigated the mechanisms of oceanic uptake of CO<sub>2</sub> (Fig. 5), which has important feedbacks to climate change under overshoot scenarios. At the highest level, known uptake mechanisms can be categorized as either biotic or abiotic. We first quantify the role of biology by comparing GENIE runs with and without biology (i.e., no biological production of

organic matter at the surface and no vertical transport of particulate organic carbon by sinking). Unlike in previous models' runs where atmospheric CO<sub>2</sub> was emitted (Figs. 1–4), here we prescribed the atmospheric CO<sub>2</sub> to follow the combination of observations and S650 that produced our control CO<sub>2</sub> emissions profile. We chose to prescribe atmospheric CO<sub>2</sub> concentrations rather than use CO<sub>2</sub> emissions so that CO<sub>2</sub> radiative forcing and thus climate are the same in the two experiments.

Fig. 5a shows that atmosphere-to-ocean CO<sub>2</sub> flux with biology (solid line) is greater than without (dashed). This is expected and reassuring, since the importance of biologically mediated, vertical transport of carbon from the surface ocean to the deep ocean in reducing atmospheric CO<sub>2</sub> level is well established since the pioneering work of Volk and Hoffert (1985). Our interest is in

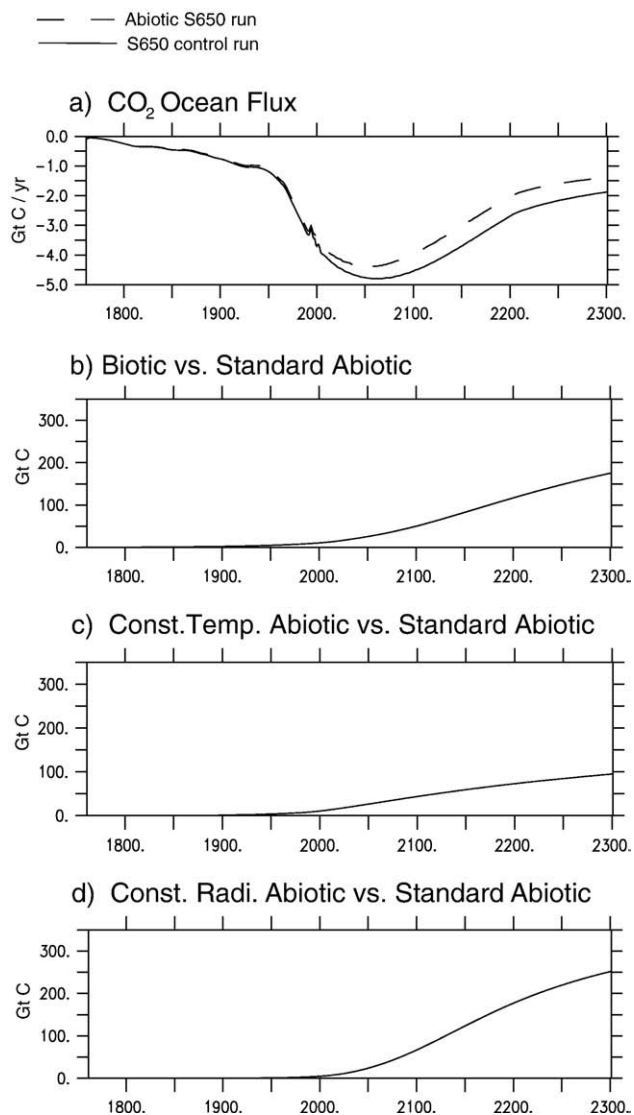


Fig. 5. Contributions to anthropogenic CO<sub>2</sub> uptake by the oceans. (a) Air-to-ocean CO<sub>2</sub> flux for the control, prescribed pCO<sub>2</sub> scenario with biology (solid line) and without (dashed). (b) CO<sub>2</sub> uptake due to biology is given by the difference between two lines in (a). A reduction in CO<sub>2</sub> uptake (i.e., negative uptake) under global warming due to (c) reduced solubility and (d) increased upper ocean stratification.

quantifying its importance. A comparison of the oceanic carbon inventory between the two simulations shows that the presence of biology in GENIE increases the ocean inventory by 176 Gt C by the year 2300 (Fig. 5b). Although this is arguably a significantly large amount, this difference represents only 13.6% of the total anthropogenic CO<sub>2</sub> uptake for the prescribed control simulation with biology, thus indicating that the major driver of CO<sub>2</sub> uptake is not biology as formulated in GENIE. It should be reminded that the formulation is rather simple, as the dependence of production is only on nutrient phosphate and light limitation due to the presence of sea ice.

Since biology contributes relatively little to the net CO<sub>2</sub> flux under overshoot scenarios, the main drivers of anthropogenic CO<sub>2</sub> uptake must be the abiotic processes, which include temperature

dependent gas solubility, pCO<sub>2</sub> gradient across the air–sea interface, and upper ocean stratification. The temperature dependent gas solubility actually has the effect of reducing CO<sub>2</sub> uptake under global warming, because an increase in temperature reduces gas solubility. In order to quantify the effect of solubility, we conducted another GENIE sensitivity run under the same prescribed atmospheric CO<sub>2</sub> without biology parameters, but while maintaining the initial sea surface temperatures as they relate to CO<sub>2</sub> solubility only. The physical model still undergoes global warming, because temperature change related to physics is not suppressed. Keeping the same preindustrial temperatures as they relate to solubility increases the carbon inventory in the ocean by 95 Gt C (Fig. 5c). Again, although this amount could be viewed as significant, it still only represents only 7.4% of the total anthropogenic CO<sub>2</sub> uptake for these scenarios, so the negative contribution of solubility to CO<sub>2</sub> uptake is relatively minor.

The effect of ocean stratification under global warming is to reduce the anthropogenic CO<sub>2</sub> uptake as well, because stratification slows the replacement of CO<sub>2</sub>-saturated surface waters with fresh interior waters. In order to examine this effect, we ran GENIE under the same prescribed atmospheric CO<sub>2</sub> without biology, but this time without the radiative forcing effect of atmospheric CO<sub>2</sub>. This means that the air and sea temperatures as well as ocean circulation remain the same as they did in 1760, even as atmospheric pCO<sub>2</sub> increases. In other words, this experiment removes the solubility effect and the circulation/stratification effect compared to the original prescribed atmospheric CO<sub>2</sub> run without biology. In Fig. 5d, we isolate the stratification effect on ocean carbon inventory by removing the solubility effect already quantified in Fig. 5c. The stratification effect increases the carbon inventory by 251 Gt C, which is 19.6% of the total anthropogenic CO<sub>2</sub> uptake. This means that the remaining pCO<sub>2</sub> gradient across the air–sea interface is the dominant driver of atmospheric CO<sub>2</sub> uptake by the ocean, since it must overcome the opposing effects of both solubility and stratification. This interpretation is supported by the anti-phasing between CO<sub>2</sub> emissions and CO<sub>2</sub> flux (Figs. 1a, g and 4a,g).

## 5. Discussion and conclusions

Our model results show that climate in GENIE under overshoot scenarios is reversible by the year 2300, which is when cumulative CO<sub>2</sub> emissions converge for the emissions scenarios considered here. That is, regardless of the different emissions histories, atmospheric pCO<sub>2</sub>, ocean and surface air temperature, air–sea CO<sub>2</sub> flux, surface ocean pH, and large scale ocean overturning circulations are nearly the same by the year 2300. This is due largely to the fact that the emissions peak occurred 244 years before the year 2300 and that this duration afforded enough time for the climate to approach equilibrium. Nakashiki et al. (2006) and Tsutsui et al. (2007) note that 100+ years is needed after the down swing in the overshoot is complete (i.e., not after the peak itself) for the recovery to take place. Had we chosen a much earlier end point for our simulations, the final climate states would not have converged.

In model experiments not shown here, we shifted the peak CO<sub>2</sub> emissions earlier or later than the control emissions scenario along the time axis. This simply shifts the model response in proportion

to the shift in forcing. Had we delayed the peak in forcing significantly, climate in GENIE would not have converged even if we kept the end point of our simulations at the year 2300.

These experiments indicate that our perspective on time is a critical factor in the debate on overshoot scenarios. The inter-generational equity the overshoot scenarios attempt to achieve would therefore depend on how far we look to the future.

In terms of the carbon cycle, we find that much of the CO<sub>2</sub> uptake by the oceans under the overshoot scenarios is driven by the pCO<sub>2</sub> gradient across the air–sea interface. There is some lag in the ocean carbon cycle response to CO<sub>2</sub> emissions forcing given the decadal timescale of thermocline ventilation. In our moderate overshoot case, atmospheric pCO<sub>2</sub> peaks almost 60 years after the maximum CO<sub>2</sub> emissions. Peak in ocean temperature changes is further delayed by another 80 years because of the large heat capacity of seawater. Again an appropriate perspective on time regarding the overshoot scenarios has to also take these lags into account.

Perhaps the most serious concern associated with overshoot scenarios is the transient response of climate. The increase in air temperature in our moderate overshoot scenario, the one that remains within the IPCC SRES emissions scenarios, is 0.6 °C relative to the control scenario. It is important to note that this is a *mean global* increase in temperature, and so some local temperatures could be much higher. We conclude by noting two important caveats in interpreting our model results. First, we did not consider the role of terrestrial biosphere, which could further modify the transient climate response. Second, the 0.6 °C warming would be a low estimate given that GENIE has relatively low climate sensitivity (2.6 °C per doubling of pCO<sub>2</sub>).

## Acknowledgments

JN was supported by a summer REU internship program made possible by an NSF grant (EAR 0649044) to the University of Minnesota. This research was supported by the Office of Science (BER), U.S. Department of Energy grant (DE-FG02-06ER64216) to KM.

## References

- Collins, W., et al., 2006. The Community Climate System Model version 3 (CCSM3). *Journal of Climate* 19, 2122–2143.
- Cubasch, U., et al., 2001. Projections of future climate change. In: Houghton, J.T., et al. (Ed.), *Climate Change 2001: The Scientific Basis*. Contribution of Working Group I to the Third Assessment Report of the Intergovernmental Panel on Climate Change. Cambridge University Press, Cambridge, pp. 525–582.
- Edwards, N.R., Marsh, R., 2005. Uncertainties due to transport-parameter sensitivity in an efficient 3-D ocean-climate model. *Climate Dynamics* 24, 415–433.
- Forster, P., et al., 2007. Changes in atmospheric constituents and in radiative forcing. In: Solomon, S., et al. (Ed.), *Climate Change 2007: The Physical Science Basis*. Contribution of Working Group I to the Fourth Assessment Report of the Intergovernmental Panel on Climate Change. Cambridge University Press, Cambridge.
- Hansen, J., et al., 2005. Earth's energy imbalance: confirmation and implications. *Science* 308 (5727), 1431–1435.
- Huntingford, C., Lowe, J., 2007. "Overshoot" scenarios and climate change. *Science* 316, 829.
- Lenton, T.M., et al., 2007. Effects of atmospheric dynamics and ocean resolution of bi-stability of the thermohaline circulation examined using the Grid ENabled Integrated Earth system modelling (GENIE) framework. *Climate Dynamics* 29, 591–613.
- Marsh, R., et al., 2004. Bistability of the thermohaline circulation identified through comprehensive 2-parameter sweeps of an efficient climate model. *Climate Dynamics* 23, 761–777.
- Marsh, R., Hazeleger, W., Yool, A., Rohling, E.J., 2007. Stability of the thermohaline circulation under millennial CO<sub>2</sub> forcing and two alternative controls on Atlantic salinity. *Geophysical Research Letters* 34 (L03605). doi:10.1029/2006GL027815.
- Matsumoto, K., Gruber, N., 2005. How accurate is the estimation of anthropogenic carbon in the ocean? An evaluation of the DC\* method. *Global Biogeochemical Cycles* 19, GB3014. doi:10.1029/2004GB002397.
- Nakashiki, N., et al., 2006. Recovery of thermohaline circulation under CO<sub>2</sub> stabilization and overshoot scenarios. *Ocean Modelling* 15, 200–217.
- Nakicenovic, N., et al., 2000. *Special Report on Emissions Scenarios (SRES)*. Cambridge University Press, Cambridge.
- Nordhaus, W.D., 2007. Critical assumptions in the Stern Review on climate change. *Science* 317, 201–202.
- Orr, J.C., et al., 2005. Anthropogenic ocean acidification over the twenty-first century and its impact on calcifying organisms. *Nature* 437 (7059), 681–686.
- Ridgwell, A., et al., 2007. Marine geochemical data assimilation in an efficient earth system model of global biogeochemical cycling. *Biogeosciences* 4, 87–104.
- Schneider, S.H., Mastrandrea, M.D., 2005. Probabilistic assessment of "dangerous" climate change and emissions pathways. *Proceedings of the National Academy of Sciences* 102, 15728–15735.
- Takahashi, T., Broecker, W.S., Werner, S.R., Bainbridge, A.E., 1980. Carbonate chemistry of the surface waters of the world oceans. *Isotope Marine Chemistry*. Uchinda Rokakuho Publ. Co. Ltd., Tokyo, pp. 291–326.
- Tsutsui, J., et al., 2007. Long-term climate response to stabilized and overshoot anthropogenic forcings beyond the twenty first century. *Climate Dynamics* 28, 199–214.
- Volk, T., Hoffert, M.I., 1985. Ocean carbon pumps: analysis of a relative strengths and efficiencies in ocean-driven atmospheric CO<sub>2</sub> changes. In: Sundquist, E.T., Broecker, W.S. (Eds.), *The Carbon Cycle and Atmospheric CO<sub>2</sub>: Natural Variations Archean to Present*. Geophysical Monograph. American Geophysical Union, Washington, pp. 99–110.
- Wanninkhof, R., 1992. Relationship between wind speed and gas exchange over the ocean. *Journal of Geophysical Research* 97 (C5), 7373–7383.
- Wigley, T.M., Richels, R., Edmonds, J.A., 1996. Economic and environmental choices in the stabilization of atmospheric CO<sub>2</sub> concentrations. *Nature* 379, 240–243.